Journal of Neurochemistry
Lippincott Williams & Wilkins, Inc., Philadelphia

Competitive Potentiation of Acetylcholine Effects on Neuronal Nicotinic Receptors by Acetylcholinesterase-Inhibiting Drugs

Ruud Zwart, Regina G. D. M. van Kleef, *Cecilia Gotti, Chantal J. G. M. Smulders, and Henk P. M. Vijverberg

*Research Institute of Toxicology, Utrecht University, Utrecht, The Netherlands; and *CNR Center of Cellular and Molecular Pharmacology, Department of Medical Pharmacology, University of Milan, Milan, Italy*

Abstract: The effects of the acetylcholinesterase inhibitors physostigmine and tacrine on $\alpha4\beta2$ and $\alpha4\beta4$ subtypes of neuronal nicotinic acetylcholine (ACh) receptors, expressed in *Xenopus laevis* oocytes, have been investigated. In voltage-clamp experiments low concentrations of physostigmine and tacrine potentiate ion currents induced by low concentrations of ACh, whereas at high concentrations they inhibit ACh-induced ion currents. These dual effects result in bell-shaped concentration–effect curves. Physostigmine and tacrine, by themselves, do not act as nicotinic receptor agonists. The larger potentiation is observed with 10 μM physostigmine on $\alpha4\beta4$ nicotinic receptors and amounts to 70% at 1 μM ACh. The mechanism underlying the effects of physostigmine on $\alpha4\beta4$ ACh receptors has been investigated in detail. Potentiation of ACh-induced ion current by low concentrations of physostigmine is surmounted at elevated concentrations of ACh, indicating that this is a competitive effect. Conversely, inhibition of ACh-induced ion current by high concentrations of physostigmine is not surmounted at high concentrations of ACh, and this effect appears mainly due to noncompetitive, voltage-dependent ion channel block. Radioligand binding experiments demonstrating displacement of the nicotinic receptor agonist ^{125}I-epibatidine from its recognition sites on $\alpha4\beta4$ ACh receptors by physostigmine confirm that physostigmine is a competitive ligand at these receptors. A two-site equilibrium receptor occupation model, combined with noncompetitive ion channel block, accounts for the dual effects of physostigmine and tacrine on ACh-induced ion currents. It is concluded that these acetylcholinesterase-inhibiting drugs interact with the ACh recognition sites and are coagonists of ACh on $\alpha4$-containing nicotinic ACh receptors. **Key Words:** Neuronal nicotinic acetylcholine receptor—Acetylcholinesterase inhibitor—Tacrine—Physostigmine—Two-site receptor occupation model—*Xenopus* oocyte.
J. Neurochem. **75,** 2492–2500 (2000).

Alzheimer's disease is accompanied by a severe deficiency of the neurotransmitter acetylcholine (ACh) in the brain (Bartus et al., 1982; Perry, 1986). In brains from patients who suffered from Alzheimer's disease it has been found that $\alpha4$ subunit-containing nicotinic ACh receptors (nAChRs) are selectively lost (Warpman and Nordberg, 1995; Martin-Ruiz et al., 1999). One strategy to improve cognitive function in Alzheimer's patients aims to enhance nicotinic neurotransmission in the brain, e.g., through elevation of the brain concentration of ACh by centrally acting acetylcholinesterase inhibitors. Physostigmine and tacrine were among the first drugs used for this purpose (reviewed by: Giacobini, 1998; Feldman and Grundman, 1999; Kelly, 1999). Other studies indicate that selective agonists of nAChRs also improve cognitive function in animal models (Lloyd and Williams, 2000), supposedly by enhancing brain nAChR function.

The exact mechanism by which the cholinesterase inhibitors enhance nicotinic neurotransmission has remained subject to debate. Apart from inhibiting acetylcholinesterases, high concentrations of physostigmine and tacrine interact directly with neuronal nAChRs (Perry et al., 1988). Ion flux studies on *Torpedo* electrocyte membrane vesicles (Okonjo et al., 1991) and single channel patch-clamp studies on rat myoballs (Maelicke et al., 1993), cultured rat hippocampal neurons (Pereira et al., 1993), mouse fibroblast (M10) cells stably transfected with chicken $\alpha4\beta2$ nAChRs (Pereira et al., 1994), and rat pheochromocytoma (PC12) cells (Storch et al., 1995) have shown that galanthamine and physostigmine activate nAChR channels. The physostigmine- and galanthamine-activated single-channel events are blocked by a monoclonal antibody (FK1) raised against the rat muscle nAChR but not by competitive nAChR antago-

Received March 27, 2000; revised manuscript received July 17, 2000; accepted July 20, 2000.

Address correspondence and reprint requests to Dr. H. P. M. Vijverberg at Research Institute of Toxicology, Utrecht University, P.O. Box 80.176, NL-3508 TD Utrecht, The Netherlands. E-mail: H.Vijverberg@ritox.vet.uu.nl

The present address of Dr. R. Zwart is Eli Lilly and Co. Ltd., Erl Wood Manor, Sunninghill Road, Windlesham, Surrey GU20 6PH, U.K.

Abbreviations used: ACh, acetylcholine; nAChR, nicotinic acetylcholine receptor.

nists. From these results, it has been concluded that physostigmine and galanthamine interact with an allosteric site on the nAChRs and act as weak partial, noncompetitive agonists at nicotinic receptors (Storch et al., 1995; Schrattenholz et al., 1996). However, there are also indications that cholinesterase inhibitors act via the agonist recognition sites of nAChRs. In *Xenopus* oocytes expressing fetal-type rat muscle nAChRs, α-bungarotoxin blocks single-channel events induced by physostigmine, galanthamine, and their methyl derivatives, suggesting a competitive rather than an allosteric effect of these drugs (Cooper et al., 1996). In whole-cell voltage-clamped insect neurons, physostigmine evokes macroscopic ion currents, which are blocked by competitive antagonists of the nAChRs (van den Beukel et al., 1998). Although physostigmine, galanthamine, and neostigmine potentiate agonist-induced whole-cell responses mediated by rat neuronal nAChRs (Schrattenholz et al., 1996; Nagata et al., 1997; Zwart et al., 1999), they fail to induce macroscopic currents in the whole-cell configuration.

In view of the apparent controversy concerning the allosteric or competitive nature of the interaction of cholinesterase inhibitors with nAChRs, we have investigated the effects of tacrine and physostigmine on rat $\alpha4\beta2$ and on $\alpha4\beta4$ nAChRs heterologously expressed in *Xenopus* oocytes. The results from voltage-clamp experiments, ligand binding experiments, and receptor modeling demonstrate that the potentiating effects are accounted for by a competitive mechanism.

MATERIALS AND METHODS

Materials

Xenopus laevis frogs were obtained from AmRep (Breda, The Netherlands) and kept in our laboratory. ACh chloride, physostigmine hemisulfate salt, and neomycin were obtained from Sigma (St. Louis, MO, U.S.A.). Tacrine hydrochloride (9-amino-1,2,3,4-tetrahydroacridine hydrochloride) was from Research Biochemicals International (Natick, MA, U.S.A.). ^{125}I-Epibatidine (2,200 Ci/mmol) was from NEN (Boston, MA, U.S.A.).

Receptor expression

Oocytes were prepared, and cDNAs encoding rat nAChR $\alpha4$ (Goldman et al., 1987) and $\beta2$ (Deneris et al., 1988) or $\beta4$ (Duvoisin et al., 1989) subunits were injected into the nucleus at a 1:1 α:β ratio as described previously (Zwart and Vijverberg, 1997). Transfected oocytes were incubated at 19°C for 3–7 days in modified Barth's solution containing 88 m*M* NaCl, 1 m*M* KCl, 2.4 m*M* $NaHCO_3$, 0.41 m*M* $CaCl_2$, 0.33 m*M* $Ca(NO_3)_2$, 0.82 m*M* $MgSO_4$, 15 m*M* HEPES, and 5 mg/L neomycin (pH 7.6 with NaOH).

Electrophysiology

Oocytes were placed in a silicon rubber tube (i.d. 3 mm), penetrated by two microelectrodes, and voltage-clamped at −40 mV, unless otherwise indicated. Voltage-clamp equipment, experimental protocols, and data acquisition were exactly as described before (Zwart and Vijverberg, 1997). Concentrated stock solutions of ACh chloride, physostigmine hemisulfate, and tacrine hydrochloride were prepared in distilled water. Dilutions of these drugs in external saline were applied to the oocytes by perfusion of the tube at a rate of ~20 ml/min. The external saline contained 115 m*M* NaCl, 2.5 m*M* KCl, 1 m*M* $CaCl_2$, and 10 m*M* HEPES (pH 7.2 with NaOH).

Preparation of oocyte homogenates

Batches of 50 frozen oocytes expressing $\alpha4\beta4$ nAChRs were thawed, homogenized in phosphate-buffered saline containing 2 m*M* phenylmethylsulfonyl fluoride using an Ultraturrax homogenizer, and subsequently diluted to 50 ml in the same buffer. The homogenates were centrifuged at 30,000 *g* at 4°C for 30 min. The dilution and centrifugation step was repeated, and the homogenates were resuspended in a buffer containing 50 m*M* Tris-HCl, 150 m*M* NaCl, 5 m*M* KCl, 1 m*M* $MgCl_2$, and 2.5 m*M* $CaCl_2$ (pH 7; buffer A). To prevent possible proteolysis during the incubation time of the assays, a mixture of the protease inhibitors leupeptin, bestatin, pepstatin A, and aprotinin (5 μg/ml each) and 2 m*M* phenylmethylsulfonyl fluoride were added to the homogenate. Receptor expression ranged from 33 to 76 fmol/mg of protein, which corresponds to an average number of nAChRs from 0.5 to 2 fmol per oocyte.

^{125}I-Epibatidine binding

Preliminary time course experiments were performed before saturation and competition analyses to determine the time required for ^{125}I-epibatidine to reach equilibrium with the $\alpha4\beta4$ nAChRs. Incubation times applied were more than four times longer to be confident of having reached equilibrium. In the epibatidine saturation experiments, aliquots of oocyte homogenates were incubated overnight at 4°C with concentrations of ^{125}I-epibatidine ranging between 0.005 and 1.6 n*M* diluted in buffer A and supplemented with 2 mg/ml bovine serum albumin. Nonspecific binding was determined in parallel by means of incubation in the presence of 250 n*M* unlabeled epibatidine. At the end of the incubation, the samples were filtered on GFC filters presoaked in polyethylenimine through a Brandel apparatus, and the filters were counted for radioactivity in a β counter. To test the ability of physostigmine to inhibit ^{125}I-epibatidine binding, physostigmine was dissolved in buffer A just before use, and serial dilutions were preincubated for 30 min at room temperature with homogenates containing $\alpha4\beta4$ nAChRs. Subsequently, a final concentration of 0.25 n*M* ^{125}I-epibatidine was added for overnight incubation at 4°C.

Electrophysiological data analysis

Amplitudes of ion currents were measured and normalized to the amplitude of ACh-induced control responses, which were evoked alternately, to adjust for differences in receptor expression levels between oocytes and for small variations in response amplitude over time. Concentration–effect curves were fitted to the data obtained in separate experiments, and mean ± SD values of estimated parameters were calculated for n oocytes. Standard activation and inhibition curves were fitted according to the following equations:

$$i/i_{max} = 1/[1 + (EC_{50}/[agonist])^{n_H}] \quad (1)$$

$$i/i_{max} = 1/[1 + ([antagonist]/IC_{50})^{n_H}] \quad (2)$$

The apparent affinity of ACh was estimated from the concentration–effect data by fitting an equilibrium model for two-site receptor occupation:

$$i/i_{max} = [cA/(1 + cA)]^2 \quad (3)$$

The two-site model (Fig. 1) applied to equilibrium effects of ACh in the presence of physostigmine or tacrine is described by Zwart and Vijverberg (1997):

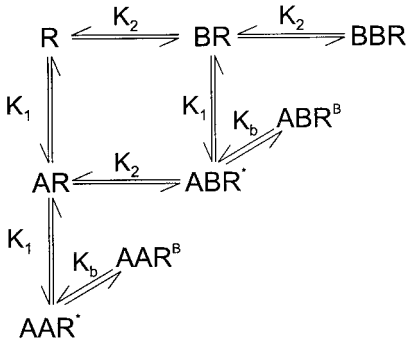

FIG. 1. Eight-state model to explain the equilibrium effects of ACh and physostigmine or ACh and tacrine on $\alpha4\beta2$ and $\alpha4\beta4$ nAChRs. This model assumes two identical agonist recognition sites that need to be occupied by ligands with agonist properties to produce a response. R, receptor; ligand A, ACh; ligand B, physostigmine or tacrine; K_1, affinity of ACh for the agonist recognition site; K_2, affinity of physostigmine or tacrine for the agonist recognition site; K_b, affinity of physostigmine or tacrine for ion channel block. Occupation of two agonist recognition sites by ACh (AAR*) and occupation of one site by ACh and the second site by physostigmine or tacrine (ABR*) result in activated receptor states from which ion channels may open with an efficacy dependent on receptor occupation. The conformational change from the fully occupied to the open states is omitted. Occupation of all agonist recognition sites by physostigmine or tacrine (BBR) does not lead to an activated receptor, and open ion channels may be blocked by physostigmine or tacrine (AAR^B and ABR^B). The ion current amplitude as a function of steady-state occupancy of the AAR* and ABR* states is described by Eq. 4 multiplied by a single-site inhibition curve (Eq. 2) to account for ion channel block by physostigmine and tacrine.

$$i_{A,B}/i_{A,0} = (1 + 2 \cdot f \cdot cB/cA) \cdot [(1 + cA)/(1 + cA + cB)]^2 \quad (4)$$

In Eqs. 3 and 4 cA and cB are the concentrations of ACh and physostigmine or tacrine, respectively, divided by their K_a values. In Eq. 4 the term $2 \cdot f \cdot cB/cA$ represents the contribution of receptors occupied simultaneously by ACh and physostigmine or ACh and tacrine to the response. The factor f accounts for the difference in efficacy of the agonist ACh (efficacy = 1) and of the combination of ACh and physostigmine or tacrine (efficacy = f). Noncompetitive channel block was accounted for by fitting the product of an agonist concentration–effect curve (Eq. 1, 3, or 4) and a single-site inhibition curve (Eq. 2; $n_H = 1$). Curve fitting was performed using Jandel Sigmaplot version 3.0 software.

Ligand binding data analysis

The experimental data obtained from the saturation binding experiments were analyzed by means of a nonlinear least squares procedure using the LIGAND program as described before (Munson and Rodbard, 1980; Gotti et al., 1998). The binding parameters were calculated by fitting the saturation data. An "extra sum of squares" F test was performed by the LIGAND program to evaluate the different binding models statistically, i.e., one-site versus two-site models, comparison of the binding parameters, etc. (Munson and Rodbard, 1980). The K_i value of physostigmine was determined by means of LIGAND, using the data obtained from three independent competition experiments.

RESULTS

Agonist effects of ACh, physostigmine, and tacrine

Superfusion of voltage-clamped oocytes expressing $\alpha4\beta2$ nAChRs with the agonist ACh results in nAChR-mediated ion currents. Oocytes expressing $\alpha4\beta2$ nAChRs have been superfused with various concentrations of ACh, and the peak amplitudes of the ACh-induced ion currents have been measured and plotted against ACh concentration. The peak amplitude of the ACh-induced ion current increased with ACh concentration up to 1 m*M* and decreased at higher agonist concentrations (Fig. 2). A decrease at very high agonist concentrations is commonly observed for nAChR-mediated ion current and is attributed to channel block by the agonist itself. Therefore, the product of a standard activation curve (Eq. 1) multiplied by a single-site inhibition curve (Eq. 2) was fitted to the data. The mean concentration–effect curve of ACh (Fig. 2; solid line) was calculated from the curves fitted to data obtained from separate oocytes (n = 3). This procedure gives reliable estimates for EC_{50}, n_H, and E_{max} values. An estimate of the apparent functional affinity of ACh for $\alpha4\beta2$ nAChRs has been obtained by fitting a two-site equilibrium receptor occupation model (Eq. 3) multiplied with a single-site inhibition curve (Eq. 2) to the same data (Fig. 2, dashed line). Previously, the same parameters have been estimated from ACh concentration–effect curves in oocytes expressing $\alpha4\beta4$ nAChRs under identical experimental conditions (Zwart and Vijverberg, 1997). The parameter estimates for $\alpha4\beta2$ and $\alpha4\beta4$ nAChRs are summarized in Table 1.

Agonist effects of physostigmine and tacrine on $\alpha4\beta2$ and $\alpha4\beta4$ nAChRs were also investigated. Oocytes expressing $\alpha4\beta2$ nAChRs and $\alpha4\beta4$ nAChRs, which responded to superfusion with 1 m*M* ACh with large

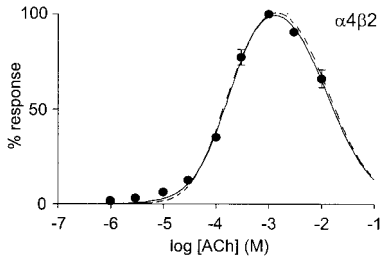

FIG. 2. Concentration–effect curve of ACh for $\alpha4\beta2$ nAChRs. Peak amplitudes of inward currents evoked by a range of ACh concentrations were normalized to the peak amplitude of the 1 m*M* ACh-induced inward current. Data are mean ± SD (bars) values for three oocytes plotted against ACh concentration. The solid line represents the fit of the mean concentration–effect curve (Eq. 1) multiplied by a single-site inhibition curve (Eq. 2) to correct for open channel block by ACh. The calculated mean values of the parameters estimated from the three experiments are shown in Table 1. The dashed line represents the mean concentration–effect curve obtained by fitting the two-site receptor occupation model (Eq. 3) including channel block to the same data. The apparent affinity (K_1) of ACh for the agonist recognition site was estimated to be 77 ± 2 μM (n = 3).

TABLE 1. *Parameter values estimated from the ACh concentration–effect curves for α4β2 and α4β4 nAChRs*

	α4β2	α4β4[a]
EC_{50} (μM)	176 ± 17	42 ± 18
n_H	1.3 ± 0.1	1.1 ± 0.3
E_{max} (%)	119 ± 4	103 ± 3
IC_{50} (m*M*)	12 ± 1	55 ± 22
K_I (μM)	77 ± 2	17 ± 9
E_{max} (%)	125 ± 1	102 ± 4
IC_{50} (m*M*)	11.1 ± 0.2	43 ± 24

Estimates for the EC_{50} for ion current activation, n_H, E_{max}, and the IC_{50} for ion channel block by ACh were obtained by fitting a standard concentration–effect curve (Eq. 1) multiplied by a single inhibition curve (Eq. 2) to the data as presented in Fig. 2. From the same data, the apparent affinity of ACh (K_I), E_{max}, and IC_{50} were estimated by fitting a two-site equilibrium receptor occupation model (Eq. 3) multiplied with a single-site inhibition curve (Eq. 2) to the data. E_{max} values are normalized to the peak inward currents induced by 1 m*M* ACh for α4β2 and by 100 μ*M* ACh for α4β4 nAChRs. Data are mean ± SD values of three oocytes.

[a] From Zwart and Vijverberg (1997).

inward currents, were also superfused with 10, 100, and 1,000 μ*M* tacrine and with 10, 100, and 1,000 μ*M* physostigmine. No inward currents were observed on superfusion with physostigmine and tacrine, demonstrating that these compounds are not α4β2 and α4β4 nAChR agonists.

Physostigmine and tacrine potentiate and inhibit ion currents evoked by low ACh concentrations

Various concentrations of physostigmine and tacrine have been applied during ion currents induced by low concentrations of ACh. Low concentrations of physostigmine and tacrine potentiate nAChR-mediated ion currents, whereas higher concentrations inhibit nAChR-mediated ion currents. An example of the effects of 0.1–100 μ*M* tacrine on 3 μ*M* ACh-induced ion currents mediated by α4β2 nAChRs is shown in Fig. 3a. On application and removal of high concentrations of tacrine, inward current transients were observed. These overshoots are attributed to the rise and fall in tacrine concentration during wash-in and wash-out and corresponding changes in tacrine effects. In addition to the effect of drug dilution, reversal of ion channel block may have contributed to the overshoot observed on removal of tacrine. Tacrine has similar effects on α4β4 nAChRs, and physostigmine has similar effects on α4β2 and α4β4 nAChRs. Steady-state effects of physostigmine and tacrine were defined as the steady current amplitude in the presence of physostigmine or tacrine relative to the control current level. The resulting bell-shaped concentration–effect curves of physostigmine and tacrine on α4β2 and α4β4 nAChR-mediated ion currents are depicted in Fig. 3b.

Although the effects of physostigmine and tacrine are qualitatively similar for both the α4β2 and α4β4 subunit combinations, the effect of physostigmine on α4β4 nAChR-mediated ion currents is the stronger effect observed. Therefore, the mechanism of potentiation has been investigated in detail for the combination of physostigmine and α4β4 nAChRs.

Potentiation by physostigmine is a surmountable effect while inhibition is a nonsurmountable effect

At the maximal effective concentration of 10 μ*M*, physostigmine potentiates α4β4 nAChR-mediated ion current evoked by 1 μ*M* ACh to 170 ± 23% (n = 3). To

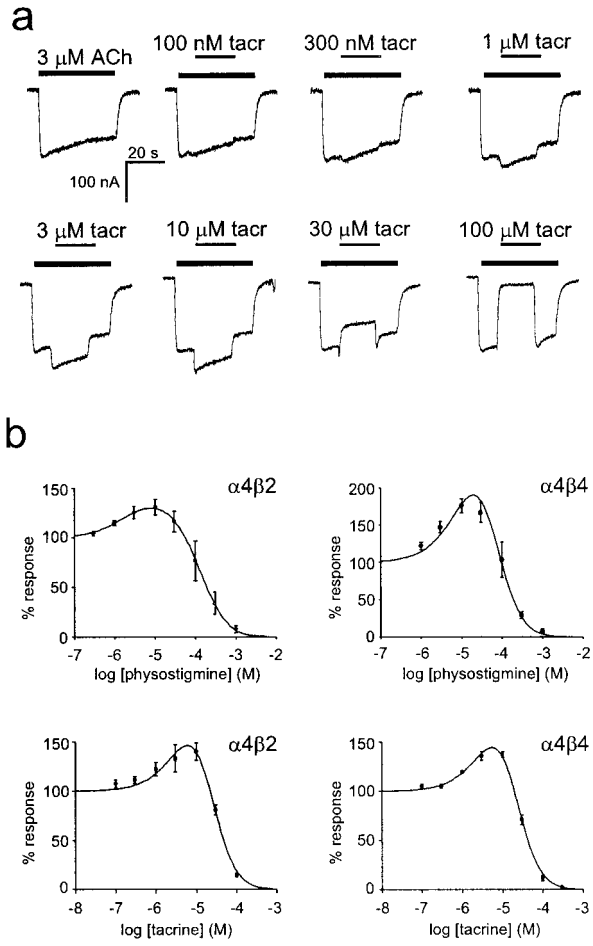

FIG. 3. Concentration dependence of physostigmine and tacrine (tacr) effects on α4β2 and α4β4 nAChR-mediated ion currents. **a:** Effects of various concentrations of tacr on α4β2 nAChR-mediated ion currents induced by 3 μ*M* ACh. The two different horizontal bars indicate the applications of 3 μ*M* ACh and the applications of tacrine at the concentrations indicated. **b:** Bell-shaped concentration dependence of the steady-state effects of physostigmine and tacrine on α4β2 and α4β4 nAChR-mediated ion currents. Ion currents were evoked with 3 μ*M* ACh for α4β2 nAChRs and with 1 μ*M* ACh for α4β4 nAChRs. Steady-state effects were determined as the steady current level in the presence of physostigmine or tacrine relative to the current level just before physostigmine or tacrine application. Data are mean ± SD (bars) values for three oocytes. The curves drawn represent the fit of the two-site equilibrium receptor occupation model (Fig. 1) to the data. In the case of physostigmine effects on α4β4 nAChRs, the curve drawn represents the simultaneous fit of the model to the data presented in Figs. 3b, 4, and 5a. Note the different scaling of the concentration–effect curve of physostigmine on α4β4 nAChRs.

determine whether potentiation by physostigmine is competitive or noncompetitive, the effect of 10 μM physostigmine has also been examined on ion currents evoked by higher agonist concentrations. The magnitude of potentiation caused by 10 μM physostigmine decreases to 133 ± 5% (n = 3) when the agonist concentration is increased to 3 μM ACh (Fig. 4a). A further increase of the ACh concentration to ≥10 μM causes a reversal of the potentiating effect of physostigmine into inhibition. This result demonstrates that at elevated agonist concentrations the potentiating effect of physostigmine is surmounted, indicating that the potentiation is due to a competitive interaction of physostigmine and ACh with the nAChRs. Conversely, the inhibitory effect of physostigmine, which remains at concentrations of ≥30 μM ACh, is not surmounted by ACh up to a concentration of 1 mM (Fig. 4b), indicating that inhibition of the ACh-induced ion current by physostigmine is due to a noncompetitive effect.

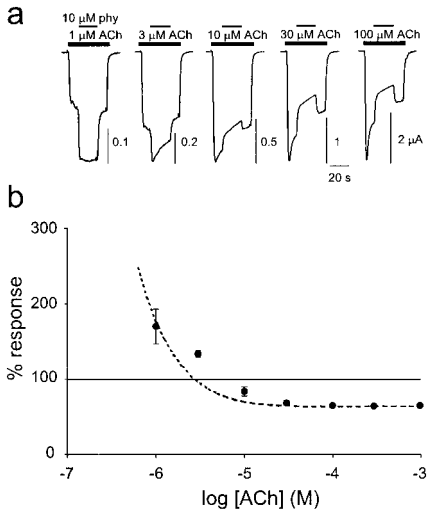

FIG. 4. Effect of ACh concentration on effect of physostigmine (phy) on $\alpha 4\beta 4$ nAChR-mediated ion current. **a:** Effects of 10 μM physostigmine on ion currents evoked by 1, 3, 10, 30, and 100 μM ACh. The two different horizontal bars indicate the applications of ACh at the concentrations indicated and the applications of 10 μM physostigmine. Physostigmine potentiates the 1 μM ACh-induced ion currents. The potentiating effect of 10 μM physostigmine is reduced when the ACh concentration is increased to 3 μM. At concentration of >3 μM ACh, the physostigmine effect is reversed, and physostigmine inhibits the ACh-induced ion current. All currents were obtained from the same oocyte and have been scaled to the same maximum. Vertical calibrations are all in μA, and the horizontal calibration applies to all traces. **b:** Steady-state effects of 10 μM physostigmine on 1, 3, 10, 30, 100, and 300 μM and 1 mM ACh-induced ion currents. Because responses desensitize at high ACh concentrations, the effects have been determined as the current level at the end of coapplication relative to the maximal current obtained after washout of physostigmine. Physostigmine potentiates the ion currents induced by low concentrations of ACh and inhibits ion currents induced by high concentrations of ACh. Data are mean ± SD (bars) values for three oocytes. The dashed line represents the simultaneous fit of the receptor occupation model to the data presented in Figs. 3b (upper right panel), 4b, and 5a.

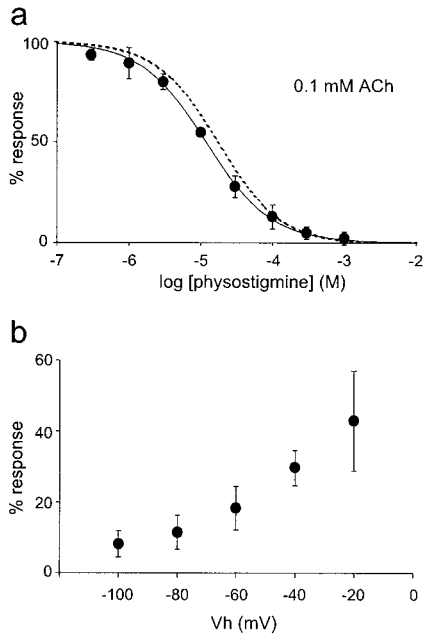

FIG. 5. Concentration- and voltage-dependent inhibition by physostigmine of $\alpha 4\beta 4$ nAChR-mediated ion currents induced by a high concentration of ACh. **a:** Concentration–effect curve for the inhibition of 0.1 mM ACh-induced responses by physostigmine. Inward current amplitudes in the presence of physostigmine were normalized to those of control inward currents induced with 0.1 mM ACh. Data are mean ± SD (bars) values for three oocytes. The solid line represents the mean concentration–effect curve calculated from the parameters estimated from fitting Eq. 2 to the data of the three experiments. The mean ± SD values obtained for the IC_{50} and n_H were 11.8 ± 0.9 μM physostigmine and 0.96 ± 0.26, respectively. The dashed line represents that predicted by the model when fitted to the data presented in Figs. 3b (upper right panel), 4b, and 5a simultaneously. **b:** Voltage dependence of 0.1 mM ACh-induced ion currents by 30 μM physostigmine. Data are mean ± SD (bars) percentages of response remaining in the presence of physostigmine in four oocytes. At each holding potential (V_h), the current amplitude was normalized to that of the 0.1 mM ACh-induced current recorded in the absence of physostigmine.

As potentiation by physostigmine is reversed into inhibition at elevated agonist concentrations, the concentration-dependent effects of physostigmine on ion currents evoked by the high concentration of 0.1 mM ACh have also been investigated (Fig. 5a). It should be noted that 0.1 mM ACh is the near-maximal effective concentration for $\alpha 4\beta 4$ nAChRs (Zwart and Vijverberg, 1997). Control 0.1 mM ACh-induced ion currents were evoked, and the effect of physostigmine was investigated by applying various concentrations of physostigmine 1 min before coapplication of physostigmine with 0.1 mM ACh. Subsequently, the oocyte was washed with external saline until complete recovery of the 0.1 mM ACh-induced ion current was obtained. At the high concentration of 0.1 mM ACh, only inhibition by physostigmine is observed. Fitting an inhibition curve (Eq. 2) to the data yielded estimates of IC_{50} and n_H of 12 ± 1 μM physostigmine and 0.96 ± 0.26, respectively. The inhibitory

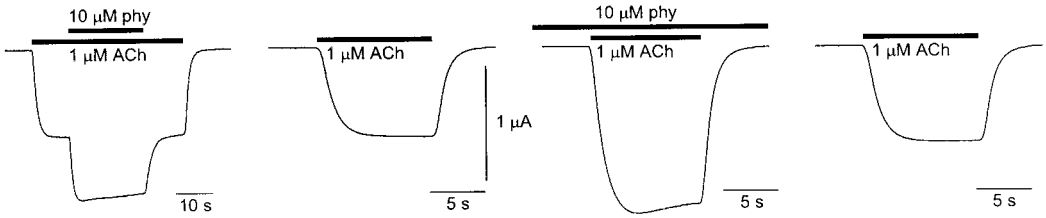

FIG. 6. Absence of slow effects of physostigmine (phy) on $\alpha4\beta4$ nAChRs. The potentiation of the 1 μM ACh-induced ion current by 10 μM physostigmine on coapplication with ACh is the same as that observed after preincubation with 10 μM physostigmine for 10 min. The four traces represent, from left to right, effect of physostigmine on coapplication, control, effect of physostigmine after a 10-min preincubation, and reversal of this effect after 10 min of washing with external solution. The responses were recorded from the same oocyte in the order shown at ~10-min intervals. A slight "run-up" of the amplitude of the control responses was observed.

effect of 30 μM physostigmine on 0.1 mM ACh-induced ion currents is voltage-dependent (Fig. 5b). The inhibition is strongest at hyperpolarized membrane potentials, and the degree of inhibition is reduced at more depolarized potentials. The voltage dependence of inhibition indicates that physostigmine blocks open nAChR ion channels.

To check whether physostigmine causes additional slow effects on the $\alpha4\beta4$ nAChR, drug coapplication was compared with preincubation. Figure 6 shows that 10 μM physostigmine potentiates the ACh-induced inward current to the same extent on coapplication with 1 μM ACh for 20 s during the agonist-induced inward current and after superfusion for 10 min before coapplication with 1 μM ACh. The results from two paired observations show that the coapplication produced 66 and 68% potentiation and the preincubation produced 68 and 72% potentiation, respectively.

Physostigmine displaces ^{125}I-epibatidine from its binding site

The surmountability of the potentiating effect of physostigmine by increasing the agonist concentration (Fig. 4) indicates that physostigmine and ACh interact with the same sites of the nAChR. Radioligand binding experiments have been performed to provide evidence that physostigmine interacts with the agonist recognition sites. ^{125}I-Epibatidine has been chosen as the radioligand because epibatidine is a high-affinity agonist for nAChRs (Badio and Daly, 1994; Parker et al., 1998). Saturation binding experiments showed that ^{125}I-epibatidine has a K_D value of 0.331 nM (coefficient of variation = 38%) and a B_{max} value of 58 ± 13 fmol/mg of protein (mean ± SEM). Analysis of the specific binding data yielded linear Scatchard plots, demonstrating the presence of a single class of high-affinity epibatidine binding sites in oocytes expressing $\alpha4\beta4$ nAChRs (Fig. 7a). Nonspecific binding, determined in parallel by means of incubation in the presence of 250 nM unlabeled epibatidine, amounted to 20–45% of total binding. No specific ^{125}I-epibatidine binding was found in untransfected oocytes. Specific ^{125}I-epibatidine binding to oocyte homogenates was displaced by physostigmine in competition binding experiments (Fig. 7b). The physostigmine concentrations used ranged from 1 nM to 1 mM. The K_i value determined from three independent duplicate experiments was 40 μM physostigmine (coefficient of variation = 31%).

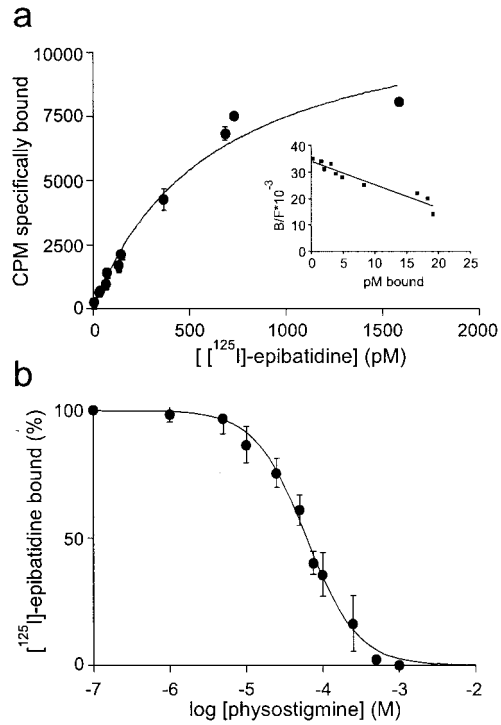

FIG. 7. Physostigmine displaces ^{125}I-epibatidine from its binding site. **a:** Saturation of specific ^{125}I-epibatidine binding to homogenates of oocytes expressing $\alpha4\beta4$ nAChRs. **Inset:** Scatchard analysis of ^{125}I-epibatidine specific binding. *B/F,* bound/free. The homogenates were incubated overnight with ^{125}I-epibatidine (0.005 and 1.6 nM) at 4°C. Nonspecific binding was determined in the presence of 250 nM epibatidine. Data are mean ± SEM (bars) values from one experiment performed in duplicate. **b:** Displacement of ^{125}I-epibatidine by physostigmine. Homogenates of oocytes expressing $\alpha4\beta4$ nAChRs were incubated with 0.25 nM ^{125}I-epibatidine overnight in the presence of the indicated concentrations of physostigmine. Data are mean ± SD (bars) values of three experiments, each performed in duplicate.

TABLE 2. *Apparent affinities of physostigmine and tacrine for the agonist binding site (K_2) and for ion channel block (K_b) and the efficacies of these drugs as coagonists (f) relative to ACh (f = 1) estimated by fitting the two-site equilibrium receptor occupation model including open channel block (Fig. 1; Eq. 4 multiplied by Eq. 2) to the data*

	$\alpha4\beta2$		$\alpha4\beta4$	
	Physostigmine[a]	Tacrine[a]	Physostigmine[b]	Tacrine[a]
K_2 (μM)	257	24	97	18
f	3.5	0.17	0.62	0.20
K_b (μM)	2.1	14	20	19

The apparent affinities of ACh (K_1) were fixed to 77 μM for $\alpha4\beta2$ nAChRs and to 17 μM for $\alpha4\beta4$ nAChRs (see Table 1).

[a] Values obtained by fitting the model to the data presented in Fig. 3b.

[b] Values obtained by fitting the model to the data presented in Figs. 3b, 4b, and 5a.

A two-site receptor occupation model accounts for the effects of physostigmine and tacrine on neuronal nAChRs

The effects of physostigmine and tacrine on $\alpha4\beta2$ and $\alpha4\beta4$ nAChR-mediated ion currents strongly resemble those reported previously for *d*-tubocurarine and atropine on neuronal nAChRs (Cachelin and Rust, 1994; Zwart and Vijverberg, 1997). The latter effects have been accounted for by a two-site receptor occupation model (Fig. 1; Eq. 4), combined with open channel block (Eq. 2). Muscle-type nAChRs have been demonstrated to possess two distinct agonist binding sites located at the α/γ and α/δ subunit interfaces (for review, see Karlin and Akabas, 1995). We have assumed that the neuronal-type nAChRs investigated have two identical binding sites because they are composed of a single type of α and a single type of β subunit and because distinct binding sites have not been demonstrated for neuronal nAChRs thus far. For the effects of physostigmine on $\alpha4\beta4$ nAChRs, the model was fitted to the data depicted in Figs. 3b, 4, and 5a. For the effects of physostigmine on $\alpha4\beta2$ nAChRs and for the effects of tacrine on $\alpha4\beta2$ and $\alpha4\beta4$ nAChRs, the model was fitted to the data depicted in Fig. 3b. The K_1 value of ACh was assumed to be 77 μM for $\alpha4\beta2$ nAChRs and 17 μM for $\alpha4\beta4$ nAChRs (see Table 1). The curves drawn in Fig. 3b and the dashed curves drawn in Figs. 4b and 5a are the result of this fitting procedure. The model predicts the potentiation and inhibition of ACh-induced ion currents by physostigmine and tacrine, as well as the changes in the nature of the effects of physostigmine dependent on the concentration of ACh. The estimated values for the parameters (K_2, f, and K_b) obtained by the nonlinear regressions are presented in Table 2.

DISCUSSION

The results demonstrate that physostigmine enhances ACh-induced ion currents in *Xenopus* oocytes expressing $\alpha4\beta4$ nAChRs by a competitive interaction with the agonist recognition sites. This conclusion is based on the surmountability of the potentiating effect by elevating the concentration of ACh (Fig. 4), the displacement by physostigmine of ^{125}I-epibatidine from the agonist recognition sites (Fig. 7), and the close fit of a two-site equilibrium receptor occupation model (Fig. 1) to the data on the potentiating and inhibitory effects of physostigmine (Figs. 3b, 4, and 5a). The close fit of the similar effects of physostigmine on $\alpha4\beta2$ nAChRs and of tacrine on $\alpha4\beta2$ and $\alpha4\beta4$ nAChRs (Fig. 3b) by the two-site model suggests that they potentiate the action of ACh at these neuronal nAChRs by a similar competitive mechanism of action. Partial agonist effects cannot account for the potentiation of ACh-induced responses because physostigmine and tacrine fail to induce detectable ion currents in *Xenopus* oocytes expressing large numbers of $\alpha4\beta2$ and $\alpha4\beta4$ nAChRs. As physostigmine and tacrine do not activate the nAChRs by themselves but enhance the action of the agonist ACh in a competitive manner, it is concluded that they are competitive coagonists of ACh at $\alpha4$-containing nAChRs.

The effects of physostigmine and tacrine observed in the present study are very similar to those reported for galanthamine and neostigmine on native neuronal nAChRs in rat pheochromocytoma PC12 cells (Schrattenholz et al., 1996; Nagata et al., 1997). However, there is a notable difference in the interpretation of the results. The results of previous studies indicate that physostigmine and galanthamine act as noncompetitive agonists at a site that is distinct from the agonist binding site of nAChRs in PC12 cells (Storch et al., 1995; Schrattenholz et al., 1996). Conversely, the present results demonstrate that physostigmine competes with epibatidine for the agonist binding site of $\alpha4\beta4$ nAChRs heterologously expressed in *Xenopus* oocytes and that the functional effects of physostigmine and tacrine are accounted for by a competitive receptor model combined with noncompetitive ion channel block. The effects of physostigmine and tacrine are also very similar to those of the competitive nAChR "antagonist" *d*-tubocurarine (Cachelin and Rust, 1994; Steinbach and Chen, 1995) and of the muscarinic ACh receptor antagonist atropine (Zwart and Vijverberg, 1997) on nAChRs. For all of these com-

pounds it has been shown that potentiation occurs only at low concentrations of ACh, whereas at high agonist concentrations the potentiation is surmounted and reversed into inhibition. This indicates that different classes of cholinergic agents are competitive coagonists of ACh at nAChRs. Other drugs potentiate nAChR-mediated responses both at low and at high agonist concentrations, e.g., flufenamic acid on rat $\alpha 3\beta 4$ nAChRs (Zwart et al., 1995) and ivermectin on chick $\alpha 7$ nAChRs (Krause et al., 1998), indicating that they act at an allosteric site.

Apart from enhancing nAChR-mediated ion currents by a competitive mechanism, high concentrations of acetylcholinesterase inhibitors also inhibit ACh-induced ion currents by a nonsurmountable blocking effect (Fig. 4). The inhibition of $\alpha 4\beta 4$ nAChR-mediated ion currents by physostigmine is voltage-dependent (Fig. 5), suggesting a mechanism of open channel block. The effects of physostigmine appear to reach equilibrium rapidly (Fig. 6), unlike the effects of neostigmine on nAChRs in PC12 cells for which increasing block was observed during repeated drug applications (Nagata et al., 1997). For muscle-type nAChRs it has been established before that physostigmine acts as an open ion channel blocker (Wachtel, 1993; Bufler et al., 1996). In the absence of channel block, a maximal potentiation of $\alpha 4\beta 4$ nAChR-mediated ion current by a factor of 7 could theoretically have been achieved at $\sim 100\ \mu M$ physostigmine (data not shown). However, because the apparent affinity of physostigmine for the channel blocking site is higher than the apparent affinity for the agonist recognition site (Table 2), the potentiation does not exceed a factor of 1.7 (Fig. 3b). The results obtained from the model show that the differences between the apparent affinities for the agonist recognition site and for ion channel block are much smaller for tacrine than for physostigmine (Table 2). This indicates that channel block plays a less prominent role in the inhibitory effect of tacrine. However, the potentiating effect of tacrine is smaller because it appears to act as a relatively low efficacy coagonist (Table 2). This raises the interesting perspective that compounds may exist that combine a high coagonist efficacy and a low channel blocking potency and that would produce large potentiating effects over a wider range of concentrations.

The present results demonstrate that drugs inhibiting acetylcholinesterases also enhance neuronal nicotinic neurotransmission by acting directly on the agonist recognition sites of $\alpha 4$ subunit-containing nAChRs. Optimal enhancement of nAChR-mediated ion currents by physostigmine and tacrine occurs at concentrations between 10 and 30 μM. IC_{50} values reported for the inhibition of acetylcholinesterases by physostigmine and tacrine vary largely, but reported values for rat brain are $<10^{-6}\ M$ (Perry et al., 1988; Xiao et al., 1993). Residual acetylcholinesterase activity of rat striatal synaptosomes treated with 30 μM physostigmine or with 30 μM tacrine amounts to 2–2.5% (Clarke et al., 1994). Although it is unknown how much residual acetylcholinesterase activity is required to maintain nicotinic neurotransmission in the CNS, the data indicate that maximal inhibition of acetylcholinesterase and maximal potentiation of nAChR function occur at similar concentrations. Recently, second-generation acetylcholinesterase inhibitors have been introduced onto the market and are being developed for the treatment of symptoms caused by Alzheimer's disease (Kelly, 1999). Whether these novel drugs exert a similar combination of effects on acetylcholinesterases and on neuronal nAChRs as observed for physostigmine and tacrine remains to be established.

Acknowledgment: We thank Dr. Jim Patrick (Baylor College of Medicine, Houston, TX, U.S.A.) for the gift of the cDNA clones of nAChR subunits, John Rowaan for taking care of the frogs, Ing. Aart de Groot for expert technical assistance, Dr. Milena Moretti for her help with the binding experiments, and Dr. Francesco Clementi for critically reading and commenting on the manuscript. This work was supported by the Netherlands Organization for Scientific Research grant 903-42-066 (to R.Z.) and the European Programme Training and Mobility of Researchers contract ERB FMRX CT97 0138 (to H.P.M.V.).

REFERENCES

Badio B. and Daly J. W. (1994) Epibatidine, a potent analgetic and nicotinic agonist. *Mol. Pharmacol.* **45,** 563–569.

Bartus R. T., Dean R. L., Beer B., and Lippa A. S. (1982) The cholinergic hypothesis of geriatric memory dysfunction. *Science* **217,** 408–414.

Bufler J., Franke C., Parnas H., and Dudel J. (1996) Open channel block by physostigmine and procaine in embryonic-like nicotinic receptors of mouse muscle. *Eur. J. Neurosci.* **8,** 677–687.

Cachelin A. B. and Rust G. (1994) Unusual pharmacology of (+)-tubocurarine with rat neuronal nicotinic acetylcholine receptors containing $\beta 4$ subunits. *Mol. Pharmacol.* **46,** 1168–1174.

Clarke P. B. S., Reuben M., and El-Brizi H. (1994) Blockade of nicotinic responses by physostigmine, tacrine and other cholinesterase inhibitors in rat striatum. *Br. J. Pharmacol.* **111,** 695–702.

Cooper J. C., Gutbrod O., Witzeman V., and Methfessel C. (1996) Pharmacology of the nicotinic acetylcholine receptor from fetal rat muscle expressed in *Xenopus* oocytes. *Eur. J. Pharmacol.* **309,** 287–298.

Deneris E. S., Connolly J., Boulter J., Wada E., Wada K., Swanson L. W., Patrick J., and Heinemann S. (1988) Primary structure and expression of $\beta 2$: a novel subunit of neuronal nicotinic acetylcholine receptors. *Neuron* **1,** 45–54.

Duvoisin R. M., Deneris E. S., Patrick J., and Heinemann S. (1989) The functional diversity of the neuronal nicotinic acetylcholine receptors is increased by a novel subunit: $\beta 4$. *Neuron* **3,** 487–496.

Feldman H. and Grundman M. (1999) Symptomatic treatments for Alzheimer's disease, in *Clinical Diagnosis and Management of Alzheimer's Disease* (Gauthier S., ed), pp. 249–268. Martin Dunitz, London.

Giacobini E. (1998) Cholinesterase inhibitors for Alzheimer's disease therapy: from tacrine to future applications. *Neurochem. Int.* **32,** 413–419.

Goldman D., Deneris E., Luyten W., Kochhar A., Patrick J., and Heinemann S. (1987) Members of a nicotinic acetylcholine receptor gene family are expressed in different regions of the mammalian central nervous system. *Cell* **48,** 965–973.

Gotti C., Balestra B., Moretti M., Rovati G. E., Maggi L., Rossoni G., Berti F., Villa L., Pallavicini M., and Clementi F. (1998) 4-Oxystilbene compounds are selective ligands for neuronal nicotinic α-bungarotoxin receptors. *Br. J. Pharmacol.* **124,** 1197–1206.

Karlin A. and Akabas M. H. (1995) Toward a structural basis for the function of nicotinic acetylcholine receptors and their cousins. *Neuron* **15,** 1231–1244.

Kelly J. S. (1999) Alzheimer's disease: the tacrine legacy. *Trends Pharmacol. Sci.* **20,** 127–129.

Krause R. M., Buisson B., Bertrand S., Corringer P. J., Galzi J. L., Changeux J. P., and Bertrand D. (1998) Ivermectin: a positive allosteric effector of the α7 neuronal nicotinic acetylcholine receptor. *Mol. Pharmacol.* **53,** 283–294.

Lloyd G. K. and Williams M. (2000) Neuronal nicotinic acetylcholine receptors as novel drug targets. *J. Pharmacol. Exp. Ther.* **292,** 461–467.

Maelicke A., Coban T., Schrattenholz A., Schroder B., Reinhardt-Maelicke S., Storch A., Godovac-Zimmermann J., Methfessel C., Pereira E. F. R., and Albuquerque E. X. (1993) Physostigmine and neuromuscular transmission. *Ann. NY Acad. Sci.* **681,** 140–154.

Martin-Ruiz C. M., Court J. A., Molnar E., Lee M., Gotti C., Mamalaki A., Tsouloufis T., Tzartos S., Ballard C., Perry R. H., and Perry E. K. (1999) α4, but not α3 and α7 nicotinic acetylcholine receptor subunits are lost from the temporal cortex in Alzheimer's disease. *J. Neurochem.* **73,** 1635–1640.

Munson P. J. and Rodbard D. (1980) LIGAND: a versatile computerized approach for characterization in agonist binding affinity. *Anal. Biochem.* **107,** 220–239.

Nagata K., Huang C. S., Song J. H., and Narahashi T. (1997) Direct actions of anticholinesterases on the neuronal nicotinic acetylcholine receptor channels. *Brain Res.* **769,** 211–218.

Okonjo K. O., Kuhlmann J., and Maelicke A. (1991) A second pathway of activation of the *Torpedo* acetylcholine receptor channel. *Eur. J. Biochem.* **200,** 671–677.

Parker M. J., Beck A., and Luetje C. W. (1998) Neuronal nicotinic receptor β2 and β4 subunits confer large differences in agonist binding affinity. *Mol. Pharmacol.* **54,** 1132–1139.

Pereira E. F. R., Reinhardt-Maelicke S., Schrattenholz A., Maelicke A., and Albuquerque E. X. (1993) Identification and functional characterization of a new agonist site on nicotinic acetylcholine receptors of cultured hippocampal neurons. *J. Pharmacol. Exp. Ther.* **265,** 1474–1491.

Pereira E. F. R., Alkondon M., Reinhardt S., Maelicke A., Peng X., Lindstrom J., Whiting P., and Albuquerque E. X. (1994) Physostigmine and galanthamine: probes for a novel binding site on the α4β2 subtype of neuronal nicotinic acetylcholine receptors stably expressed in fibroblast cells. *J. Pharmacol. Exp. Ther.* **270,** 768–778.

Perry E. K. (1986) The cholinergic hypothesis—ten years on. *Br. Med. Bull.* **42,** 63–69.

Perry E. K., Smith C. J., Court J. A., Bonham J. R., Rodway M., and Atack J. R. (1988) Interaction of 9-amino-1,2,3,4-tetrahydroaminoacridine (THA) with human cortical nicotinic and muscarinic receptor binding in vitro. *Neurosci. Lett.* **91,** 211–216.

Schrattenholz A., Pereira E. F. R., Roth U., Weber K. H., Albuquerque E. X., and Maelicke A. (1996) Agonist responses of neuronal nicotinic acetylcholine receptors are potentiated by a novel class of allosterically acting ligands. *Mol. Pharmacol.* **49,** 1–6.

Steinbach J. H. and Chen Q. (1995) Antagonist and partial agonist actions of *d*-tubocurarine at mammalian muscle acetylcholine receptors. *J. Neurosci.* **15,** 230–240.

Storch A., Schrattenholz A., Cooper J. C., Abdel Ghani E. M., Gutbrod O., Weber K. H., Reinhardt S., Lobron C., Hermsen B., Soskic V., Pereira E. F. R., Albuquerque E. X., Methfessel C., and Maelicke A. (1995) Physostigmine, galanthamine and codeine act as 'non-competitive nicotinic receptor agonists' on clonal rat phaeochromocytoma cells. *Eur. J. Pharmacol.* **290,** 207–219.

van den Beukel I., Van Kleef R. G. D. M., Zwart R., and Oortgiesen M. (1998) Physostigmine and acetylcholine differentially activate nicotinic receptor subpopulations in *Locusta migratoria* neurons. *Brain Res.* **789,** 263–273.

Wachtel R. E. (1993) Physostigmine block of ion channels activated by acetylcholine in BC3H1 cells. *Mol. Pharmacol.* **44,** 1051–1055.

Warpman U. and Nordberg A. (1995) Epibatidine and ABT 418 reveal selective losses of α4β2 nicotinic receptors in Alzheimer brains. *Neuroreport* **6,** 2419–2423.

Xiao W. B., Nordberg A., and Zhang X. (1993) Effect of *in vivo* microdialysis of 1,2,3,4-tetrahydro-9-aminoacridine (THA) on the extracellular concentration of acetylcholine in the striatum of anesthetized rats. *J. Pharmacol. Exp. Ther.* **265,** 759–764.

Zwart R. and Vijverberg H. P. M. (1997) Potentiation and inhibition of neuronal nicotinic receptors by atropine: competitive and non-competitive effects. *Mol. Pharmacol.* **52,** 886–895.

Zwart R., Oortgiesen M., and Vijverberg H. P. M. (1995) Differential modulation of α3β2 and α3β4 neuronal nicotinic receptors expressed in *Xenopus* oocytes by flufenamic acid and niflumic acid. *J. Neurosci.* **15,** 2168–2178.

Zwart R., van Kleef R. G. D. M., and Vijverberg H. P. M. (1999) Physostigmine and atropine potentiate and inhibit neuronal α4β4 nicotinic receptors. *Ann. NY Acad. Sci.* **868,** 636–639.